GEOPHYSICAL RESEARCH LETTERS, VOL. 19, NO. 15, PAGES 1607-1610, AUGUST 3, 1992

CLIMATE FORCING BY STRATOSPHERIC AEROSOLS

Andrew Lacis, James Hansen and Makiko Sato

NASA Goddard Space Flight Center, Goddard Institute for Space Studies, New York

Abstract. We illustrate how climate forcing by stratospheric aerosols depends on aerosol properties. The climate forcing is a function of aerosol size distribution, but the size dependence can be described well by a single parameter: the area-weighted mean radius, r_{eff}. If r_{eff} is greater than about 2 μm, the global average greenhouse effect of the aerosols exceeds the albedo effect, causing a surface heating. The aerosol climate forcing is less sensitive to other characteristics of the size distribution, the aerosol composition, and the altitude of the aerosols. Thus stratospheric aerosol forcing can be defined accurately from measurements of aerosol extinction over a broad wavelength range.

Introduction

Volcanic aerosols have long been speculated to be an important mechanism for climate change. Humphreys (1940) attempted quantitative analyses, assessing both the aerosol's albedo effect, which cools the Earth by reducing absorption of sunlight, and the aerosol's greenhouse effect, which warms the Earth by absorbing upwelling terrestrial radiation. Humphreys' results greatly exaggerated the aerosol cooling tendency, because he assumed incorrectly that aerosols scatter mainly in the backward direction, and he underestimated their greenhouse effect, because he assumed incorrectly that the aerosols behaved as Rayleigh particles in the thermal infrared region.

Radiative transfer tools are now available for accurate simulation of climate forcing by aerosols. Coakley and Grams (1976), Harshvardhan and Cess (1976), and Pollack et al. (1976) were among the first to realistically portray the effect of stratospheric aerosols on both solar and terrestrial radiation. While most investigators made calculations for a specific aerosol composition and size distribution, Coakley and Grams (1976) considered the full range of particle sizes, showing that both very small particles (radius $r < 0.05$ μm) and large particles ($r > 1$ μm) could cause surface heating, while particles of intermediate size usually cause surface cooling. Hansen et al. (1980) and Pollack et al. (1981) illustrated how the radiative forcing varied as a function of aerosol composition, size and altitude. Nevertheless, it is difficult to sort out the relative importance of different aerosol parameters and some uncertainty persists. For example, Pollack et al. (1981) argue that even a very small amount of absorption by stratospheric aerosols can change the sign of the climate forcing, greatly complicating observational requirements.

In this paper we examine how stratospheric aerosol climate forcing depends upon aerosol parameters. This should help specify needed aerosol observations and define uncertainties in the aerosol forcing for climate impact studies.

Aerosol Climate Forcing

Techniques for calculating aerosol scattering, including gaseous absorption in a vertically inhomogeneous atmosphere, are well developed. Our single scattering calculations use Mie theory for spheres as described by Hansen and Travis (1974). The multiple scattering is based on the doubling and adding methods for a plane-parallel atmosphere as described by Lacis and Hansen (1974). Gaseous absorption is included using the correlated k-distribution method [Lacis and Oinas, 1990]. Temperature changes are computed with the one-dimensional radiative-convective (1-D RC) model of Lacis et al. (1981), which is designed for global mean conditions with 50% cloud cover and 6.5°C/km tropospheric lapse rate. Although aerosol climate forcing varies with latitude and season, the aerosols from climatically significant volcanos generally spread over at least a hemisphere and remain airborne about a year or more. Thus the global (or hemispheric) mean is an appropriate case for studying the dependence of the forcing on aerosol parameters.

Sample single and multiple scattering results are shown in Figure 1 for aerosols composed of a 75% sulfuric acid solution in water, for optical parameters measured by Palmer and Williams (1975). Results are illustrated for two size distributions, "May" and "October" particles, measured by Hofmann and Rosen (1983) 1½ and 6½ months after the eruption of El Chichon in 1982. The May size distribution contained more large particles (radius $\gtrsim 1$ μm), which increase absorption of thermal radiation. King et al. (1989) have shown results similar to parts of Figure 1 for three size distributions.

Figure 2(a) shows the solar and thermal components of the global radiative forcing due to sulfuric acid aerosols of optical depth 0.1 ($\lambda = 0.55$ μm) at 20-25 km altitude. We plot the

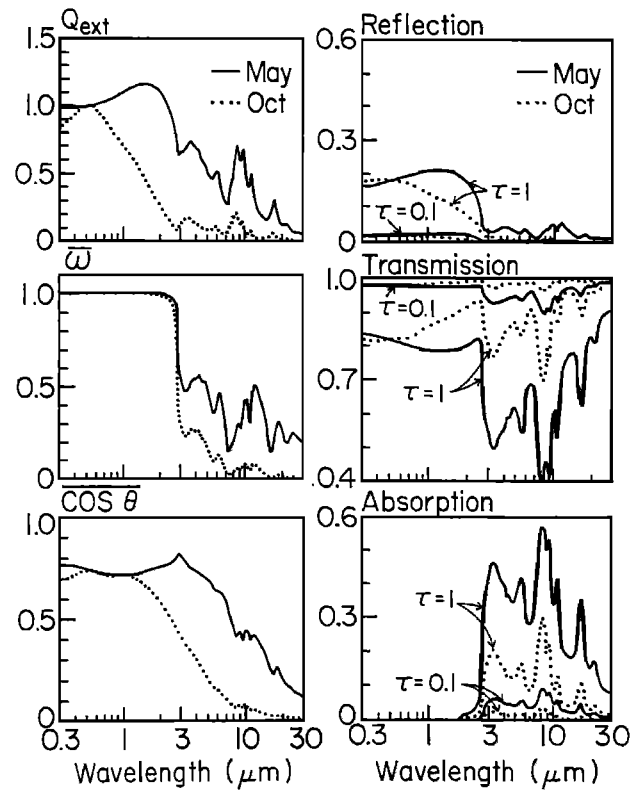

Fig. 1. Single scattering (left) and multiple scattering (right) by sulfuric acid aerosols for two size distributions measured by Hofmann and Rosen (1983). Q_{ext} is the extinction coefficient, $\tilde{\omega}$ the single scattering albedo, cos θ the single scattering asymmetry factor, R the reflectivity of a plane parallel layer of optical thickness τ (0.55 μm), A the absorption, and T the diffuse transmission [Hansen and Travis, 1974].

Paper number 92GL01620
0094-8534/92/92GL-01620$03.00

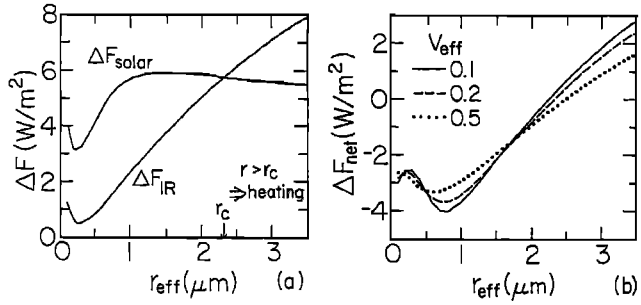

Fig. 2. (a) Change of solar and infrared fluxes at the tropopause caused by adding a stratospheric (20-25 km) aerosol layer with τ (0.55 μm) = 0.1 in a 1-D RC model with fixed surface temperature. Aerosol sizes follow the gamma distribution with v_{eff} = 0.2. (b) Change of net radiative flux at the tropopause for the same case and for two other values of v_{eff}.

decrease of downward solar flux (cooling) and the increase of downward thermal flux (warming) at the tropopause as a function of the aerosol effective radius. The effective radius [Hansen and Travis, 1974] is the mean radius of the size distribution weighted by the aerosol cross-sectional area. The fluxes were calculated for global mean conditions, using the gamma size distribution (equation 2.56 of Hansen and Travis, 1974) with effective variance 0.2; the surface (and thus tropospheric) temperature were fixed, but the stratospheric temperature was allowed to adjust to a new equilibrium profile. The flux change at the tropopause for these conditions, ΔF_{net}, is a good measure of climate forcing. For example, we show in a paper in preparation that the climate changes computed in a general circulation model for many radiative perturbations are mainly a function of this (equilibrium) tropopause flux change (with certain pathological exceptions which greatly modify the temperature profile, such as changes of the ozone profile). Multiplying ΔF_{net} by 0.3 yields the quantity ΔT_o (°C), which is another measure of climate forcing, the equilibrium surface air temperature rise which would occur in the absence of climate feedbacks [Hansen et al., 1984].

Figure 2(a) shows the infrared forcing to be a strong function of particle size, while the solar albedo effect is relatively insensitive to particle size if r_{eff} is larger than the effective solar wavelength. As a result, aerosols with critical radius $r_c \gtrsim 2$ μm lead to tropospheric *heating* for global mean conditions. We show below that this critical radius is rather insensitive to particle composition and the shape of the size distribution. Very small aerosols (r_{eff} < 0.05 μm) also cause heating [Coakley and Grams, 1976], but such small aerosols are not sufficiently abundant to be radiatively significant.

The lifetime of large stratospheric particles is limited by their settling rate. A 1 μm radius sulfuric acid droplet at 20 km altitude requires about ½ month to fall 1 km. Volcanic ash, usually less dense and more irregular in shape, may fall more slowly than sulfuric acid droplets. Aerosol size distributions measured 1½ and 6½ months after the El Chichon eruption had r_{eff} of 1.4 μm and 0.5 μm, respectively [Hofmann and Rosen, 1983]. Thus particle size affects the magnitude of the climate forcing, but only in unusual circumstances could it cause heating of the surface.

Figure 2(b) shows how the net radiative forcing (solar plus thermal) changes with the width of the particle size distribution. A broader size distribution smooths the variation of radiative forcing with effective radius, but changes only slightly the critical radius separating heating and cooling. Results for the log-normal size distribution with the same values of v_{eff} are indistinguishable from those in Figure 2(b). Hansen and Travis (1974) show that radiative quantities are also very similar for power law (Junge) and bimodal gamma distributions with the same effective radiance and variance, and they give analytic expressions relating the parameters of all four distributions to r_{eff} and v_{eff}. Thus to a good approximation the net radiative forcing depends on just two parameters of the aerosol size distribution, r_{eff} and v_{eff}, and we may use a convenient analytic function, such as the gamma distribution, to represent an arbitrary size distribution.

Figure 3 summarizes the dependence of net radiative forcing on r_{eff} and v_{eff}. r_{eff}/v_{eff} combinations of several measured size distributions are shown, but certain qualifications must be borne in mind. First, some measurement techniques have difficulty recording the small number of large particles often present; because large particles strongly influence the area-weighted integrals, r_{eff} and v_{eff} may be underestimated. Second, although very narrow size distributions occur at a given place and time, such distributions are not relevant to global climate forcing. The climate responds to radiative forcing averaged over time, and to a substantial extent, averaged over space. Such averaging probably eliminates values of $v_{eff} \lesssim 0.1$.

From Figure 3 and these considerations, it is apparent that aerosol climate forcing depends only modestly on v_{eff}. If $r_{eff} \lesssim 1$ μm the net radiative flux at the tropopause is near 3 W/m² for τ = 0.1 (λ = 0.55 μm). Thus for small τ the climate forcing due to a global stratospheric layer of sulfuric acid aerosols based on our calculations is

$$\Delta F_{net}\ (W/m^2) \sim 30\ \tau, \qquad (1)$$

or

$$\Delta T_o\ (°C) \sim 9\ \tau, \qquad (2)$$

which should apply to any volcanos of the past century ($\tau \lesssim$ 0.2). Figure 3 suggests that (1) and (2) vary $\lesssim$ 25% for 0.1 $\lesssim r_{eff} \lesssim$ 1 μm.

It is difficult to specify precisely the absolute accuracy of our results. Harshvardhan (1979) also obtained a net forcing near 3 W/m² for sulfuric acid aerosols with τ = 0.1. It would be useful to precisely define a few specific cases for comparative calculations with several independent radiative algorithms.

An important issue of aerosol composition is whether minor constituents (impurities) can significantly reduce the single scattering albedo for solar radiation ($\tilde{\omega}_c$). Pollack et al. (1981) concluded that impurities reducing $\tilde{\omega}_c$ to 0.98 or less would change the sign of climate forcing from cooling to heating.

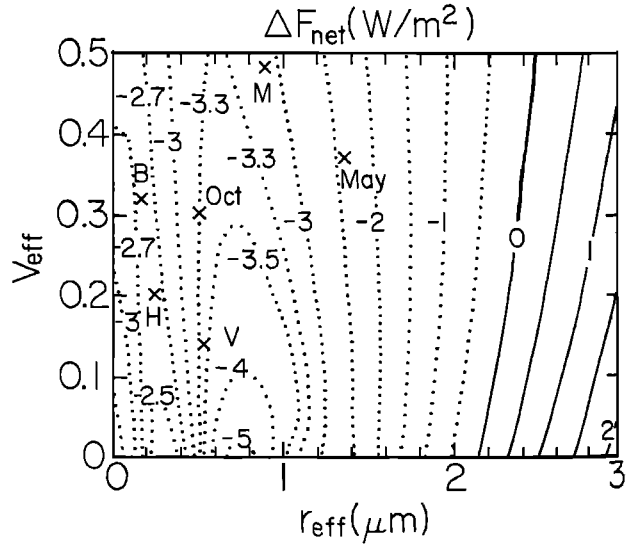

Fig. 3. Net radiative flux change at the tropopause caused by addition of a stratospheric aerosol layer with τ = 0.1 (0.55 μm) and other conditions as in Figure 2. Marked r_{eff}/v_{eff} combinations for specific aerosol size distributions: May and Oct are the 1982 observations of Hofmann and Rosen (1983), B and V are stratospheric background and volcanic size distributions reported by Oberbeck et al. (1983), and H and M are Deirmendjian (1969) haze distributions.

Should the sensitivity to impurities be so high, it would be difficult to assess the climate forcing by volcanic eruptions. For example, $\tilde{\omega}_c = 0.99$ would yield cooling only about half as large as for $\tilde{\omega}_c = 1$. It is practically impossible to measure $\tilde{\omega}_c$ from space to the accuracies implied by these numbers; even with in situ measurements it is not trivial to achieve such accuracy.

This aerosol impurity issue is addressed by Figure 4 which shows aerosol radiative forcing and equilibrium stratospheric temperature (20-25 km) for several values of $\tilde{\omega}_c$. The calculations used sulfuric acid aerosol properties except $\tilde{\omega}$ was replaced by $\tilde{\omega}_c$ at λ with $\tilde{\omega} > \tilde{\omega}_c$, basically $\lambda < 3$ μm (Fig. 1). Figure 4(a) shows that the sulfuric acid forcing of tropospheric climate is nearly independent of plausible levels of absorbing impurities, even though the impurities can cause a large increase of stratospheric heating (Fig. 4b). In fact, the added absorption slightly increases surface cooling, by reducing diffusely transmitted solar energy reaching the troposphere. The increase of downward thermal radiation due to the warmer stratosphere is not sufficient to balance the loss of solar energy absorbed in the troposphere and ground.

Because volcanic aerosols may initially contain a large proportion of ash, we illustrate in Figure 5 the dependence of radiative forcing on extreme changes of composition. Basalt optical constants [Pollack et al., 1973] are typical of silicates, a common constituent of volcanic ash. Desert dust, with optical parameters measured by Volz (1973), is an example of a substance with strong absorption of solar radiation. The climate forcing is greater for basalt and dust than for sulfuric acid (Fig. 5a). This can be traced to (1) the larger real refractive indices of basalt and dust, which increase the proportion of backscattered solar radiation and the optical depth in the 0.55-2 μm region relative to the optical depth at 0.55 μm, and (2) the absorption by basalt and dust, which reduces the amount of scattered radiation reaching the troposphere.

Figure 5(b) shows major differences in the temperature change of the aerosol layer (20-25 km). The equilibrium heating is a strong function of r_{eff} for $r_{eff} \lesssim 1$ μm. This is because τ (near ir) and τ (ir) increase relative to τ (0.55 μm) with larger r_{eff} (Fig. 1), increasing the absorption of solar and thermal radiation. For desert dust, and for $\tilde{\omega} < 1$ in Figure 4(b), the absorption of sunlight dominates over thermal heating.

Figure 6 shows how the climate forcing and stratospheric warming depend on aerosol altitude. The dotted curve in Figure 6(a) is the instantaneous change of net radiative flux at the tropopause caused by a 1 km thick $\tau = 0.1$ aerosol layer, as a function of the altitude where the layer is added. This instantaneous flux change at the tropopause is commonly used to define climate forcing. However, the net flux change at the tropopause *after* the stratospheric temperature profile has reached radiative-convective equilibrium (with fixed surface and tropospheric temperature) is a better indicator of climate forcing, since the radiative relaxation time of the stratosphere is less than the residence time of the radiative perturber. As Figure 6(a) shows, the climate forcing thus defined is nearly independent of aerosol height in the stratosphere.

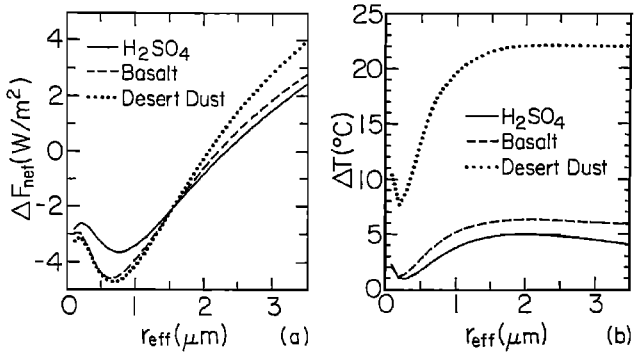

Fig. 5. Change of net radiative flux at the tropopause (a) and stratospheric temperature (b) caused by stratospheric aerosols with τ (0.55 μm) = 0.1 for the gamma size distribution with $v_{eff} = 0.2$. Results show the effect of aerosol composition.

Figure 6(b) shows the equilibrium change of temperature profile for aerosols added at different altitudes. There are competing effects because the aerosols both heat the layer where they are added, by absorbing solar and terrestrial radiation, and cool the layer, mainly by emitting thermal radiation. There is a cross-over point at about 30 km, above which aerosols cause stratospheric cooling (as well as tropospheric cooling); this is because of higher local temperature and increased efficiency for cooling to space. Aerosols injected near 30 km would be expected to have little impact on stratospheric temperatures initially. However, as the aerosols subside to lower altitudes the heating should increase.

Figure 7 (a) shows that the aerosol climate forcing as a function of visible optical depth for $\tau < 1$. Departures from linearity are caused by different rates of saturation for the solar and thermal components. Stratospheric warming begins to saturate at τ of several tenths. The larger radiative forcing for the October particles reflects the size dependence shown in Figures 2 and 3, and the greater stratospheric warming for the May particles reflects their larger infrared opacity (Figure 1).

Discussion

Several caveats are attached to the calculations reported here. The climate forcings are computed with a global mean

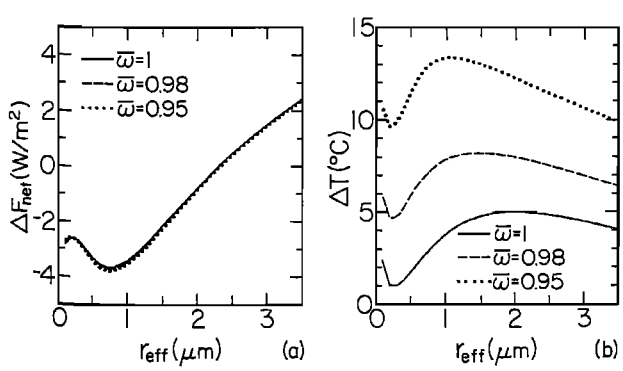

Fig. 4. Change of net radiative flux at the tropopause (a) and stratospheric temperature (b) caused by adding an aerosol layer with τ (0.55 μm) = 0.1 at 20-25 km. Results show the effect of impurities which reduce the single scattering albedo for solar radiation. The gamma size distribution is used with $v_{eff} = 0.2$.

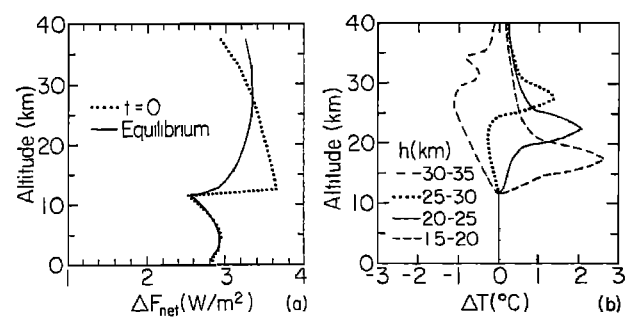

Fig. 6. (a) Change of net radiative flux at the tropopause caused by addition of a sulfuric acid aerosol layer with τ (0.55 μm) = 0.1. Instantaneous and radiative equilibrium results are shown, with the surface and tropospheric temperatures fixed. (b) Change of equilibrium temperature profile when aerosols are added to indicated layers.

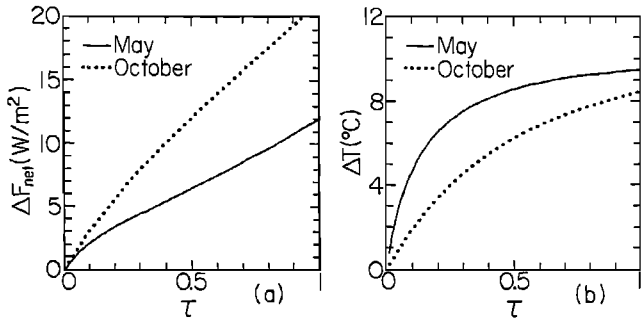

Fig. 7. Change of net radiative flux at the tropopause (a) and stratospheric temperature (b) caused by addition of aerosol layer of optical depth τ (0.55 μm) at altitudes 20-25 km for the aerosol size distributions measured by Hofmann and Rosen (1983) in May and October 1982.

radiative-convective model, with all the approximations that implies. However, we have also made some computations with a general circulation model, and do not find substantial changes. The calculations assume spherical particles, as is appropriate for the dominant sulfuric acid aerosols. But we anticipate the results being qualitatively valid for nonspherical particles as well, because the basic parameters determining the results are the optical depth and particle size.

Our main conclusion is that aerosol forcing of tropospheric climate is remarkably independent of most aerosol parameters other than optical thickness. An exception is particle size: greenhouse heating by particles larger than 1 μm can rival or exceed the albedo cooling effect, and a small fraction of such particles can influence the radiative properties of the aerosol size distribution. But other aerosol parameters, including absorption by impurities, which would be difficult to measure, are much less important. This means that it is feasible to determine accurately volcanic aerosol climate forcing from satellite measurements, and also that it should be possible to infer aerosol forcings of the past with a useful accuracy from ground-based optical extinction data.

Acknowledgements. We thank Christina Koizumi for typesetting, Jose Mendoza for drafting, Dr. Alan Robock and an anonymous referee for helpful comments, and Dr. Harshvardhan for comparisons with his radiative algorithms.

References

Coakley, J. A., and G. Grams, Relative influence of visible and infrared optical properties of a stratospheric aerosol layer on the global climate, *J. Appl. Meteorol.*, *15*, 679-691, 1976.

Deirmendjian, D., *Electromagnetic Scattering on Spherical Polydispersions*, Elsevier, New York, 290 pp., 1969.

Hansen, J. E., and L. D. Travis, Light scattering in planetary atmospheres, *Space Sci. Rev.*, *16*, 527-610, 1974.

Hansen, J. E., et al., Mount Agung provides a test of a global climatic perturbation, *Science*, *199*, 1065-1068, 1978.

Hansen, J. E., et al., Climatic effects of atmospheric aerosols, *Ann. New York Acad. Sci.*, *338*, 575-587, 1980.

Hansen, J. E., et al., Climate sensitivity: analysis of feedback processes, *Geophys. Mono. Ser.*, *29*, 130-163, 1984.

Hansen, J. E., et al., Global climate changes as forecast by the Goddard Institute for Space Studies three-dimensional model, *J. Geophys. Res.*, *93*, 9341-9364, 1988.

Harshvardhan, Perturbation of the zonal radiation balance by a stratospheric aerosol layer, *J. Atmos. Sci.*, *36*, 1274-85, 1979.

Harshvardhan, and R. D. Cess, Stratospheric aerosols: effect upon atmospheric temperature and global climate, *Tellus*, *28*, 1-10, 1976.

Hofmann, D. J., and J. M. Rosen, Sulfuric acid droplet formation and growth in the stratosphere after the 1982 eruption of El Chichon, *Science*, *222*, 325-327, 1983.

Humphreys, W. J., *Physics of the Air*, McGraw-Hill, New York, 676 pp., 1940.

King, M. D., Harshvardhan, and A. Arking, A model of the radiative properties of the El Chichon stratospheric aerosol layer, *J. Clim. Appl. Meteorol.*, *23*, 1121-1137, 1984.

Lacis, A. A., and J. E. Hansen, A parameterization for the absorption of solar radiation in the earth's atmosphere, *J. Atmos. Sci.*, *31*, 118-133, 1974.

Lacis, A. A., and V. Oinas, A description of the correlated K-distribution method, *J. Geophys. Res.*, *96*, 9027-9064, 1991.

Lacis, A. A., et al., Greenhouse effect of trace gases, 1970-1980, *Geophys. Res. Lett.*, *8*, 1035-1038, 1981.

Oberbeck, V. R., et al., Effect of the eruption of El Chichon on stratospheric aerosol size and composition, *Geophys. Res. Lett.*, *10*, 1021-1024, 1983.

Palmer, K. F., and D. Williams, Optical constants of sulfuric acid, *Appl. Optics*, *14*, 208-219, 1975.

Pollack, J. B., et al., Optical properties of some terrestrial rocks and glasses, *Icarus*, *19*, 372-389, 1973.

Pollack, J. B., et al., Volcanic explosions and climatic change: a theoretical assessment, *J. Geophys. Res.*, *81*, 1071-83, 1976.

Pollack, J. B., et al., Radiative properties of the background stratospheric aerosols and implications for perturbed conditions, *Geophys. Res. Lett.*, *8*, 26-28, 1981.

Volz, F. E., Infrared optical constants of ammonium sulfate, Sahara dust, volcanic pumice, and flyash, *Appl. Opt.*, *12*, 564-568, 1973.

A. Lacis, J. Hansen and M. Sato, Goddard Institute for Space Studies, 2880 Broadway, New York, NY 10025.

(Received: March 28, 1992;
accepted: June 24, 1992)